npj | parkinson's disease

Article

Published in partnership with the Parkinson's Foundation

https://doi.org/10.1038/s41531-026-01306-x

Ultra-performance liquid chromatography–mass spectrometry analysis of post-mortem brain tissue reveals specific amino acid profile dysregulation in Parkinson's disease and Alzheimer's disease patients

Check for updates

Jacopo Gervasoni[1,10], Anna Di Maio[2,3,10], Marcello Serra[4,10], Michela Cicchinelli[5], Lavinia Santucci[1,5], Gabriele Ciasca[5], Tommaso Nuzzo[2,3], Qin Li[6], Marie-Laure Thiolat[7], Micaela Morelli[4,8], Andrea Urbani[1,5], Francesco Errico[2,9], Erwan Bezard[6,7] & Alessandro Usiello[2,3] ✉

Previous metabolomic studies have reported significant alterations in circulating amino acids in Parkinson's disease (PD). However, it remains unclear whether these changes reflect central nervous system pathology or are restricted to peripheral metabolism. To address this issue, here we measured the levels of a panel of amino acids in *post-mortem* brain samples from MPTP-intoxicated monkeys, with and without L-DOPA treatment, and from PD patients at different Braak Lewy body (LB) stages through targeted UPLC-MS. In untreated MPTP monkeys, the putamen showed significant increases in glutamate, aspartate, GABA, phenylalanine, branched-chain amino acids, and serine. L-DOPA treatment further altered this profile, increasing glycine, threonine, and citrulline levels. In contrast, no amino acid changes were detected in the superior frontal gyrus (SFG) of MPTP monkeys, regardless of treatment. In PD patients, caudate-putamen analysis revealed consistent serine upregulation at Braak LB stages 3–4 and 6, with stage 6 additionally showing increased proline and reduced phosphoethanolamine. No amino acid changes were observed in the PD SFG, whereas Alzheimer's disease SFG samples showed marked amino acid increases. Together, these findings demonstrate region-specific amino acid dysregulation in PD, preferentially affecting nigrostriatal targets and supporting disease-specific metabolic signatures across neurodegenerative disorders.

Parkinson's disease (PD) is the second most prevalent neurodegenerative disorder after Alzheimer's disease (AD), affecting approximately 1–3% of individuals aged 60 years and older[1]. Notably, the global prevalence of PD is rising significantly, with a particularly pronounced increase observed over the past two decades[1]. Neuropathologically, PD is characterized by the loss of dopaminergic neurons in the substantia nigra pars compacta and the presence of Lewy bodies and neurites—abnormal aggregates of insoluble proteins primarily composed of α-synuclein[2].

PD is increasingly recognized as a multifactorial, systemic, and heterogeneous disorder, characterized by marked variability in motor

[1]Fondazione Policlinico Universitario A. Gemelli IRCCS, Largo Agostino Gemelli 8, Roma, Italy. [2]CEINGE Biotecnologie Avanzate Franco Salvatore, Naples, Italy. [3]Department of Environmental, Biological and Pharmaceutical Sciences and Technologies, Università degli Studi della Campania "Luigi Vanvitelli", Caserta, Italy. [4]Department of Biomedical Sciences, University of Cagliari, Monserrato, Italy. [5]Università Cattolica del Sacro Cuore, Largo Francesco Vito, 1, Roma, Italy. [6]Motac France, Floirac, France. [7]Université de Bordeaux, CNRS, IMN, UMR 5293, Bordeaux, France. [8]Neuroscience Institute, National Research Council of Italy (CNR), Cagliari Cittadella Universitaria, Monserrato, Italy. [9]Department of Agricultural Sciences, University of Naples "Federico II", Portici, Italy. [10]These authors jointly supervised this work Jacopo Gervasoni, Anna Di Maio, Marcello Serra. ✉e-mail: alessandro.usiello@unicampania.it; usiello@ceinge.unina.it

symptoms (tremor, rigidity, bradykinesia, postural instability), non-motor symptoms (hyposmia, autonomic dysfunction, sleep disturbances, cognitive impairment), and treatment response[3]. This heterogeneity poses significant challenges to clinical diagnosis— primarily dependent on clinical and neuroimaging evaluation in the 85–90% of idiopathic cases —and for treatment selection[4].

To disentangle this complex scenario, a series of putative biomarkers, encompassing clinical indicators, neuroimaging, genomics, and biomolecules, has been proposed to enhance diagnostic accuracy and monitor disease progression[5]. Notwithstanding the valuable insights these biomarkers have provided regarding aspects of patients' pathological conditions, none have yet demonstrated the specificity required to definitively diagnose PD, track disease progression, or predict treatment response[5,6].

Over the last decade, metabolomic investigation—through the comprehensive analysis of small molecules or metabolites within a biological system— has emerged as a powerful approach for elucidating the complex biochemical alterations associated with disease states. Studies conducted across different biological matrices, including serum, plasma, urine, cerebrospinal fluid (CSF), and saliva, in both animal models of PD and Parkinsonian patients, have identified numerous systemic metabolic alterations that provide valuable insights into the disease's pathophysiology[7,8]. These alterations encompass dysregulation in lipid homeostasis[9–13], mitochondrial energy metabolism[10,14–16], ammonium recycling and purine biosynthesis pathways[17–19].

Additionally, metabolomic and High-Performance Liquid Chromatography (HPLC) investigations have revealed significant alterations in the homeostasis of neuroactive D- and L-amino acids in blood serum/plasma and CSF samples from patients with PD compared to controls[9,14,20–30]. Altered amino acid profiles in PD patients are thought to reflect disruptions in protein biosynthesis, neurotransmitter homeostasis, and key cellular signaling pathways, including urea cycle function, antioxidant (e.g., glutathione) synthesis, and energy metabolism[23]. Importantly, from a multi-organ perspective, these amino acid alterations may provide critical insights into disease progression by revealing metabolic dysregulation in peripheral organs—such as the kidneys and liver—in patients with PD[31,32].

While these biochemical alterations underscore the potential for developing novel "fingerprints" for PD, they also reveal the inherent complexity of PD pathophysiology. In this regard, conflicting results and inconsistencies across studies render it challenging to draw definitive conclusions regarding the central molecular events driving these changes[33].

A key challenge that complicates mechanistic interpretation of available data is that most of the above cited metabolomic studies have been conducted using patients' peripheral biofluids, particularly plasma and serum, whereas investigations of brain tissue remain comparatively scarce, particularly in the caudate-putamen (CPu), the basal ganglia nucleus most profoundly affected by dopaminergic nigrostriatal denervation.

For instance, it is unclear whether the distinct PD signature previously identified in patients' blood also occurs centrally. Factors such as blood–brain barrier permeability, dietary influences, pharmacological treatments, systemic metabolism, and comorbid conditions can profoundly reshape peripheral metabolomic profiles, thereby complicating accurate extrapolation to the brain's metabolic state.

To clarify this outstanding issue, the present study aims to employ a targeted metabolic approach using UPLC-MS—the gold standard in clinical chemical diagnostics—to quantify and compare the levels of a broad panel of amino acids implicated in neurotransmission, oxidative stress, and mitochondrial-related energy homeostasis *in post-mortem* samples obtained from: (1) the rostral putamen and superior frontal gyrus (SFG) of 1-methyl-4-phenyl-1,2,3,6-tetrahydropyridine (MPTP)-intoxicated macaques, never exposed to L-DOPA or chronically treated with L-DOPA, and their respective controls; (2) the CPu and SFG of PD patients at different Braak Lewy body (LB) stages and matched controls; and (3) the SFG of patients with Alzheimer's disease (AD) and matched controls. Our UPLC-MS analysis revealed significant amino acid profile alterations in *post-mortem* striatal—but not cortical—samples from both MPTP-intoxicated macaques and PD patients compared to controls. These amino acid changes only partially overlap between monkeys and humans and, in PD patients, were restricted to serine, proline, and phosphoethanolamine. Lastly, we found multiple amino acid alterations in the SFG of AD patients compared to controls, suggesting a prominent role of underlying neurodegenerative pathology in the cortical amino acid profile.

Results

MPTP-induced dopamine denervation and L-DOPA treatment alter putaminal amino acid profile in macaques

First, utilizing the MPTP macaque model, considered a gold standard preclinical model of PD[34], we investigated the impact of MPTP-induced nigrostriatal dopamine degeneration and repeated L-DOPA treatment on *post-mortem* putaminal levels of a broad panel of amino acids. Specifically, we compared the amino-acid profiles of MPTP-intoxicated monkeys (i) never exposed to L-DOPA (untreated, drug-naïve; $n = 4$) and (ii) chronically treated with therapeutically relevant doses of L-DOPA (mimicking late-stage PD; $n = 5$) with those of control monkeys ($n = 5$).

UPLC-MS data revealed distinct variations in the concentrations of a subset of amino acids, an effect dependent on both MPTP-induced dopaminergic denervation and chronic L-DOPA treatment (Fig. 1A).

Based on this evidence, we conducted a univariate statistical analysis to identify amino acids differentially expressed in untreated (Fig.1B) and L-DOPA-treated (Fig.1E) MPTP-intoxicated macaques compared with controls. Statistical significance was assessed using a two-sample *t*-test, while a fold change (FC) quantified the magnitude and direction of amino acid alterations. Results are presented as volcano plots and boxplots (Fig.1C, D, F, G), revealing distinct patterns of change. In untreated MPTP-intoxicated macaques, eight amino acids were significantly upregulated compared with controls: valine (FC = 1.41; $p = 0.013$), serine (FC = 1.63; $p = 0.017$), leucine (FC = 1.41; $p = 0.022$), isoleucine (FC = 1.43; $p = 0.025$), aspartic acid (FC = 1.40; $p = 0.026$), GABA (FC = 1.52; $p = 0.033$), phenylalanine (FC = 1.43; $p = 0.034$), and glutamic acid (FC = 1.36; $p = 0.044$). In L-DOPA–treated MPTP-intoxicated macaques, a distinct set of eight amino acids was upregulated: serine (FC = 2.08; $p = 8.19 \times 10^{-4}$), glycine (FC = 1.64; $p = 0.014$), threonine (FC = 1.86; $p = 0.027$), GABA (FC = 1.70; $p = 0.015$), phenylalanine (FC = 1.52; $p = 0.016$), valine (FC = 1.60; $p = 0.037$), isoleucine (FC = 1.57; $p = 0.037$), and citrulline (FC = 1.63; $p = 0.019$). Overall, the UPLC-MS data revealed both shared and distinct alterations in putaminal amino-acid concentrations (Fig. 2). Serine, GABA, phenylalanine, valine, and isoleucine were significantly upregulated in both untreated and L-DOPA-treated MPTP-intoxicated macaques relative to controls. In contrast, leucine, aspartic acid, and glutamic acid were specifically upregulated in untreated MPTP-intoxicated monkeys, whereas glycine, citrulline, and threonine were uniquely elevated in L-DOPA-treated macaques.

A direct comparison between untreated and L-DOPA-treated MPTP-intoxicated macaques revealed a significant upregulation of citrulline in the L-DOPA-treated group (FC = 1.44; $p = 0.043$), suggesting a treatment-specific modulation of this amino acid. Detailed results are provided in Supplementary Fig. 1.

Taken together, these findings indicate that MPTP-induced dopaminergic degeneration and L-DOPA treatment elicit both overlapping and distinct alterations in the putaminal amino acid profile of the macaque model.

Amino acid profile in the superior frontal gyrus is unaffected by MPTP-induced denervation and L-DOPA treatment in macaques

Next, to determine whether the amino acid alterations observed in untreated and L-DOPA–treated MPTP-intoxicated macaques relative to controls were confined to the putamen or extended to cortical regions, we expanded our UPLC-MS analysis to the *post-mortem* superior frontal gyrus (SFG). In contrast to the putamen, no comparable pattern of amino acid variation was detected in the SFG (Fig. 3A). This observation was supported by univariate analyses, which revealed no amino acids significantly altered in either untreated

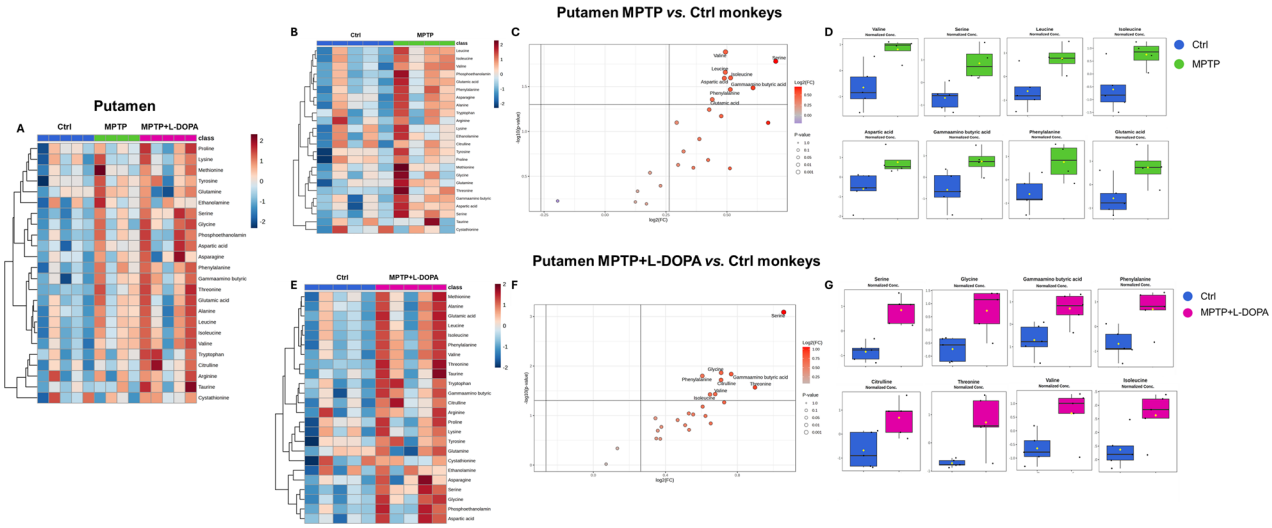

Fig. 1 | MPTP-induced dopamine degeneration and L-DOPA-treatment elicit significant amino acid alterations in the putamen of monkeys. A Heatmap showing standardized amino acid concentrations (*z*-score) across the three experimental groups (Ctrl, $n = 5$; MPTP, $n = 4$; MPTP + L-DOPA, $n = 5$). Rows represent individual amino acids and columns represent individual biological samples, highlighting the variation in amino acid levels. **B** Heatmap of amino acid concentrations for the pairwise comparison between MPTP and Ctrl groups. **C** Robust volcano plot for the MPTP *vs.* Ctrl comparison, displaying $\log_2$(FC) and $-\log_{10}$(*p*-value), with eight significantly altered amino acids highlighted. **D** Boxplots illustrating amino acids significantly upregulated in untreated MPTP monkeys relative to Ctrl. **E** Heatmap of amino acid concentrations for the pairwise comparison between MPTP + L-DOPA and Ctrl groups. **F** Robust volcano plot for the MPTP + L-DOPA *vs.* Ctrl comparison, displaying $\log_2$(FC) and $-\log_{10}$(*p*-value), with eight significantly altered amino acids highlighted. **G** Boxplots illustrating amino acids significantly upregulated in MPTP + L-DOPA monkeys relative to Ctrl. Ctrl control, MPTP 1-methyl-4-phenyl-1,2,3,6-tetrahydropyridine.

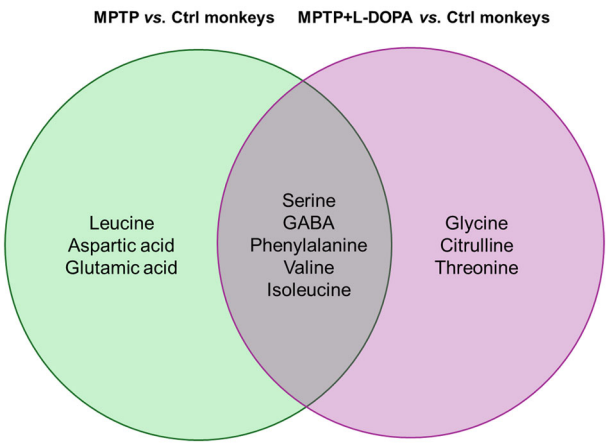

Fig. 2 | Shared and specific alterations in putaminal amino acid concentrations of untreated and L-DOPA-treated MPTP-intoxicated monkeys relative to controls. The Venn diagram illustrates the overlap between amino acids significantly upregulated in untreated MPTP-intoxicated monkeys compared with controls (green) and those upregulated in MPTP + L-DOPA-treated monkeys compared with controls (purple). Five amino acids — serine, GABA, phenylalanine, valine, and isoleucine — were commonly upregulated in both untreated and L-DOPA-treated MPTP-intoxicated monkeys relative to controls. Leucine, aspartate, and glutamate were selectively increased in MPTP-intoxicated monkeys, whereas glycine, citrulline, and threonine were selectively increased in the MPTP + L-DOPA–treated group. Ctrl control, MPTP 1-methyl-4-phenyl-1,2,3,6-tetrahydropyridine.

or L-DOPA–treated MPTP-intoxicated macaques compared to controls (Fig. 3B–E). Moreover, no significant differences in amino acid profiles were detected between untreated and L-DOPA–treated MPTP-intoxicated macaques (Supplementary Fig. 2). Collectively, these findings indicate that neither MPTP intoxication nor L-DOPA treatment induced detectable alterations in the amino acid profile of the SFG, consistent with a region-specific effect.

Parkinson's disease patients display Braak Lewy Body Stage-dependent amino acid alterations in the *post-mortem* caudate-putamen

We next investigated whether the pathological amino acid alterations observed in the putamen of untreated and L-DOPA-treated MPTP-intoxicated macaques relative to controls were also present in the *post-mortem* CPu from PD patients at different Braak LB stages. Specifically, we compared the amino-acid profile in the *post-mortem* CPu of PD patients at Braak LB stages 3–4 ($n = 13$) and stage 6 ($n = 13$) with that of non-demented controls ($n = 6$).

We first examined the amino acid profile in the CPu of all PD patients ($n = 26$) relative to controls to assess overall alterations. Univariate analyses were performed using two-sample *t*-tests to evaluate statistical significance, and fold change (FC) was used to quantify the magnitude and direction of variations. The results revealed three significantly altered amino acids in PD patients: serine (FC = 1.37; $p = 0.014$) and proline (FC = 1.28; $p = 0.04$) were upregulated, whereas phosphoethanolamine was downregulated (FC = −1.51; $p = 0.049$) relative to controls (Supplementary Fig. 3).

This assessment was followed by analyses stratified by Braak LB stage (Fig. 4A), with additional comparisons between Braak LB stages 3–4 and controls (Fig. 4B) and between stage 6 and controls (Fig. 4E) using univariate statistical analyses. Results are presented as robust volcano plots and boxplots (Fig. 4C, D, F, G), highlighting amino acids with significant alterations.

Comparisons between Braak LB stages 3–4 PD patients and controls revealed a significant upregulation of serine (FC = 1.29; $p = 0.039$) (Fig. 4D). In PD patients at Braak LB stage 6, more pronounced changes were observed, with the upregulation of serine (FC = 1.45; $p = 0.005$) and proline (FC = 1.31; $p = 0.033$), and the downregulation of phosphoethanolamine (FC = −1.54; $p = 0.046$) (Fig. 4G).

Moreover, a direct comparison between the two PD Braak LB stages (3–4 vs. 6) revealed a significant downregulation of arginine (FC = −1.29; $p = 0.03$) in stage 6 relative to stage 3–4 (Supplementary Figure 4).

Overall, these results indicate that the amino acid profile in the *post-mortem* CPu of PD patients undergoes progressive, stage-dependent alterations, with specific amino acids exhibiting greater dysregulation or emerging at advanced Braak LB stages.

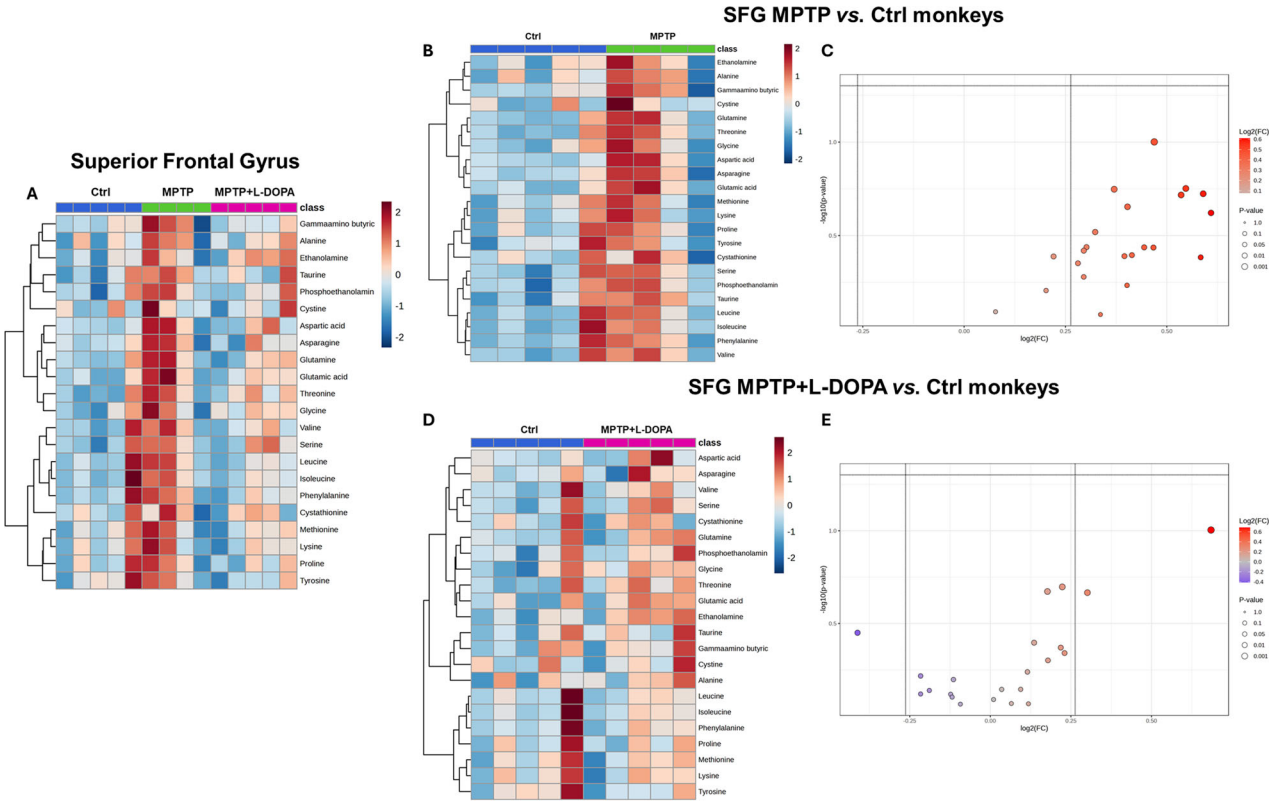

Fig. 3 | Untreated and L-DOPA-treated MPTP-intoxicated monkeys showed an unaltered amino acid profile in the superior frontal gyrus. A Heatmap showing standardized amino acid concentrations (*z*-score) across the three experimental groups (Ctrl $n = 5$, MPTP $n = 4$, MPTP + L-DOPA $n = 5$). Rows represent individual amino acids and columns represent individual biological samples, highlighting the variation in amino acid levels. **B** Heatmap of amino acid concentrations for the pairwise comparison between MPTP and Ctrl groups. **C** Robust volcano plot for the MPTP *vs.* Ctrl comparison, displaying $\log_2$(FC) and $-\log_{10}$(*p*-value) and highlighting no significant variation in amino acid levels. **D** Heatmap of amino acid concentrations for the pairwise comparison between MPTP + L-DOPA and Ctrl. **E** Robust volcano plot for the MPTP + L-DOPA *vs.* Ctrl comparison, displaying $\log_2$(FC) and $-\log_{10}$(*p*-value) and highlighting no significant variation in amino acid levels. Ctrl control, MPTP 1-methyl-4-phenyl-1,2,3,6-tetrahydropyridine, SFG superior frontal gyrus.

Parkinson's disease does not alter amino acid profiles in the post-mortem superior frontal gyrus

Using an approach analogous to that applied in the macaque model, we investigated the impact of PD on the *post-mortem* SFG by analyzing cortical amino-acid concentrations selected according to the experimental conditions. The analysis included PD patients at Braak Lewy body (LB) stages 4–5 ($n = 4$) and 6 ($n = 6$), compared with controls ($n = 10$). An initial univariate analysis was conducted to assess overall amino acid alterations in the SFG of PD patients ($n = 10$) relative to controls. Using two-sample *t*-tests to evaluate statistical significance and fold change (FC) to quantify the magnitude and direction of variations, no significant alterations were identified (Supplementary Fig. 5). This result was further supported by analyses stratified by Braak LB stage (Fig. 5A) and by pairwise comparisons between Braak LB stages 4–5 and controls (Fig. 5B, C) and between Braak LB stage 6 and controls (Fig. 5D, E). Univariate analyses revealed no significant differences in amino acid profiles across Braak LB stages relative to controls, nor in the direct comparison between Braak LB stages 4–5 and 6 (Supplementary Fig. 6).

The absence of significant variations in the *post-mortem* SFG of PD patients supports region-specific amino acid alterations, with SFG levels remaining preserved.

Overall, the results in PD patients are consistent with those of MPTP-intoxicated macaques, highlighting that amino acid dysregulation is detectable in the putamen region of both untreated and L-DOPA-treated MPTP-intoxicated macaques, as well as in the CPu region of PD patients across Braak LB stages, whereas no comparable alterations were observed in the SFG in either species. To summarize the principal findings, the Venn diagram in Fig. 6 illustrates the amino acid alterations identified in the putamen of the macaque model and in the human *post-mortem* CPu.

Despite differences between the amino acid signatures associated with MPTP intoxication and L-DOPA treatment in monkeys and those emerging across Braak LB stages in humans, serine was consistently and significantly upregulated across all univariate analyses.

Amino acid dysregulation in the *post-mortem* superior frontal gyrus of Alzheimer's disease patients

Considering the role of the superior frontal gyrus in the pathophysiology of AD[35–37] and the absence of alterations observed in the PD cohort, we investigated whether cortical amino acid changes differ significantly across distinct neurodegenerative conditions. To this end, we performed a univariate analysis of *post-mortem* SFG samples from AD patients ($n = 10$) and controls ($n = 10$), using cortical amino acid concentrations selected based on the experimental conditions.

Statistical significance was evaluated using two-sample *t*-tests and fold-change (FC) analysis. The heatmap (Fig. 7A) showed variation in amino acid concentrations between AD patients and controls, revealing distinct clusters of amino acids with similar patterns across the two groups. This finding was supported by the robust volcano plot (Fig. 7B), which highlighted five amino acids significantly upregulated in the AD group relative to controls. Specifically, tryptophan (FC = 1.37; $p = 0.002$), phenylalanine (FC = 1.34; $p = 0.003$), threonine (FC = 1.32; $p = 0.013$), tyrosine (FC = 1.27; $p = 0.022$), and methionine (FC = 1.32; $p = 0.024$). These differences were further illustrated in the corresponding boxplots (Fig. 7C).

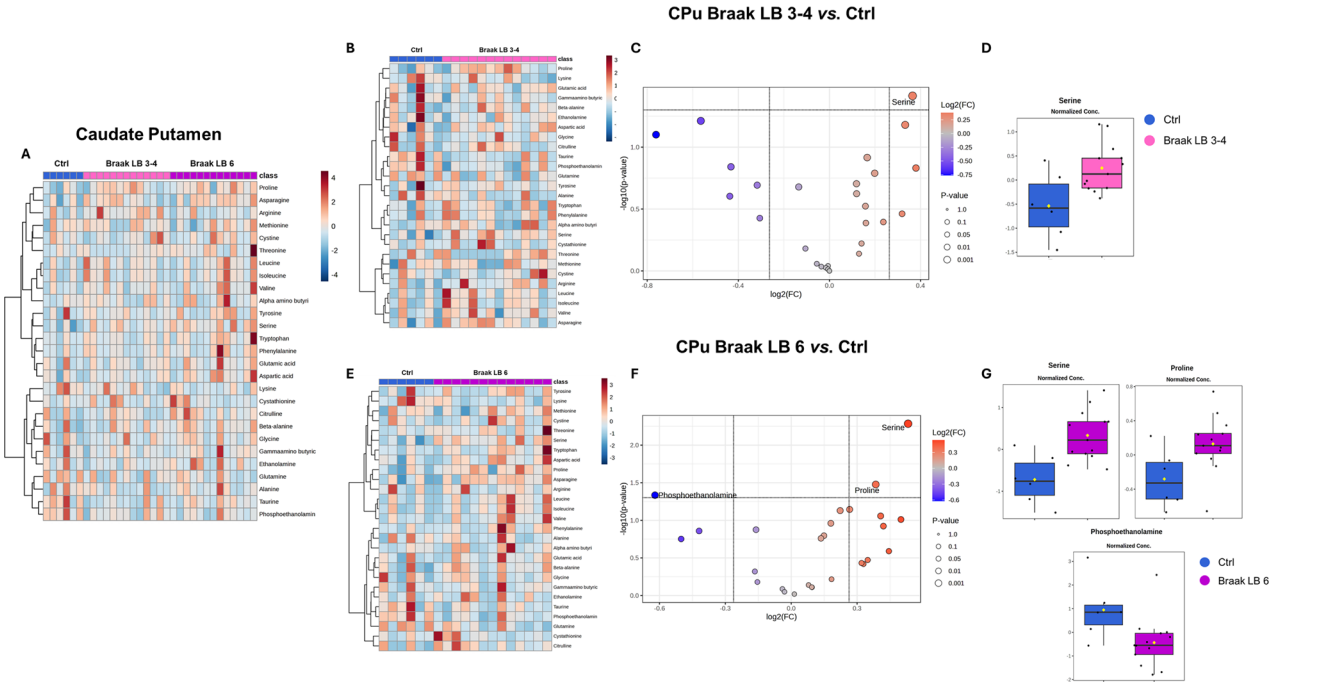

Fig. 4 | Stage-dependent amino acid variation in the *post-mortem* caudate-putamen of PD patients with respect to non-demented controls. A Heatmap showing standardized amino acid concentrations (*z*-score) across the non-demented controls (Ctrl, $n = 6$), Braak LB 3–4 ($n = 13$), and Braak LB 6 ($n = 13$) PD patients, illustrating the overall amino acid profile. Rows represent individual amino acids and columns represent individual biological samples, highlighting the variation in amino acid levels. **B** Heatmap of amino acid concentrations for the pairwise comparison between Braak LB 3–4 and Ctrl. **C** Robust volcano plot for the Braak LB 3–4 *vs.* Ctrl comparison, displaying $\log_2$(FC) and $-\log_{10}$(*p*-value) and highlighting one significant amino acid. **D** Boxplot illustrating the amino acid significantly upregulated in Braak LB 3–4 relative to Ctrl. **E** Heatmap of amino acid concentrations for the pairwise comparison between Braak LB 6 and Ctrl. **F** Robust volcano plot for the Braak LB 6 *vs.* Ctrl comparison, displaying $\log_2$(FC) versus $-\log_{10}$(*p*-value), highlighting three significantly altered amino acids. **G** Boxplots illustrating amino acids significantly upregulated in Braak LB 6 relative to Ctrl. Ctrl control, Braak LB Braak Lewy Body Stage, CPu caudate-putamen.

Discussion

Accumulating studies have revealed significant metabolic dysregulation in the peripheral biofluids—particularly plasma and serum—of PD patients relative to healthy individuals[13–15,20–24,27,38]. These alterations encompass dysregulation in amino acid metabolism, lipid homeostasis, mitochondrial energy metabolism, and purine biosynthesis pathways[7,14,33], highlighting the complex and multifactoral origin of PD[39–42]. While these studies provide key insights into the blood metabolic state of the disease, it remains uncertain whether these alterations reflect modifications in central biochemical processes—particularly within the basal ganglia—or instead reflect broader systemic disturbances.

In the present study, we employed targeted UPLC-MS—a state-of-the-art analytical method renowned for its elevated sensitivity, selectivity, and wide dynamic range—to quantify the concentrations of a broad panel of amino acids implicated in neurotransmission, oxidative stress, and mitochondrial-related energy homeostasis in *post-mortem* brain samples from MPTP-intoxicated monkeys, with or without L-DOPA treatment, patients with PD or AD, and their respective healthy controls. The primary objective was to determine whether the amino acid alterations previously reported in the CSF and blood of PD patients, by using metabolomics and HPLC determinations[7,9,14,22,23,27–30,33,38], are also detectable, or instead differ, in the CPu and SFG of PD patients at different Braak LB stages.

Furthermore, to clarify the specific role of nigrostriatal dopaminergic degeneration and L-DOPA-induced dyskinesia (LID), we extended our UPLC-MS analysis to the *post-mortem* putamen and SFG samples from MPTP-intoxicated macaques, treated with or without L-DOPA.

UPLC-MS analysis in macaques revealed significant alterations in cerebral amino acids associated with nigrostriatal pathway denervation. In the *post-mortem* putamen of untreated MPTP-intoxicated monkeys, we observed increased levels of the neurotransmitters glutamate, aspartate, and GABA, as well as phenylalanine, a dopamine precursor, compared with controls. We also detected a marked elevation of serine, which modulates N-methyl-D-aspartate (NMDA) receptor signaling through the regulation of endogenous co-agonist levels, including D-serine and glycine. Beyond these neuroactive amino acids, untreated MPTP-intoxicated macaques exhibited increased putaminal levels of the branched-chain amino acids (BCAAs) leucine, isoleucine, and valine. Notably, LID remodeled the putaminal amino acid profile. Specifically, serine, GABA, phenylalanine, valine, and isoleucine remained elevated compared with controls, indicating core metabolic disturbances that persist despite dopaminergic therapy, whereas glycine, citrulline, and threonine were elevated exclusively in L-DOPA–treated animals, consistent with treatment-dependent amino acid adaptations.

The observed alterations in the excitatory amino acids glutamate and aspartate, found exclusively in the *post-mortem* putamen of untreated MPTP-intoxicated macaques, reinforce previous evidence indicating a major role for glutamatergic dysregulation in PD pathophysiology[43–45], and aligned with previous HPLC findings from our group reporting a remarkable tendency toward increased glutamate and aspartate levels in the rostral putamen of untreated MPTP-intoxicated macaques compared to controls[46]. The absence of these changes in L-DOPA–treated MPTP-intoxicated macaques may reflect treatment-related modulation of glutamatergic tone or compensatory mechanisms induced by repeated dopaminergic stimulation. In this respect, previous *post-mortem* studies conducted in small cohorts of L-DOPA–treated PD patients have reported either no alterations in striatal glutamate and aspartate levels[47–49], or increased glutamate concentrations[50]. Future studies are needed to clarify how the concentration of these excitatory amino acids evolves during disease progression as well as after the emergence of LID, as L-DOPA may engage distinct mechanisms of action during the advanced stage of the disease[51].

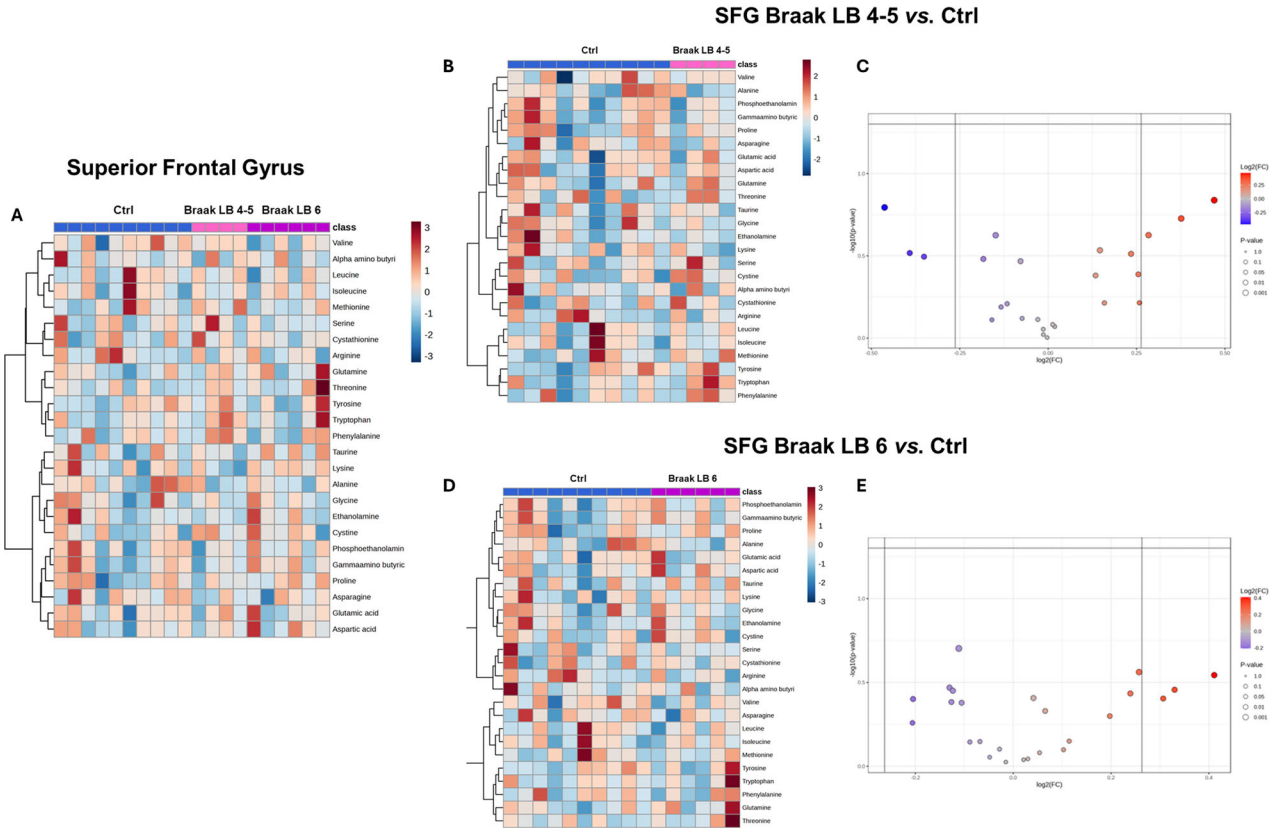

Fig. 5 | Amino acid levels in the *post-mortem* superior frontal gyrus are not affected by Parkinson's disease. A Heatmap showing standardized amino acid concentrations (*z*-score) across the non-demented controls (Ctrl, $n = 10$), Braak LB 4–5 ($n = 4$), and Braak LB 6 ($n = 6$) PD patients. Rows represent individual amino acids and columns represent individual biological samples, highlighting the variation in amino acid levels. **B** Heatmap of amino acid concentrations for the pairwise comparison between Braak LB 4–5 and Ctrl. **C** Robust volcano plot for the Braak LB 4–5 *vs.* Ctrl comparison, displaying $\log_2$(FC) and $-\log_{10}$(*p*-value) and highlighting no significant variations in amino acid levels. **D** Heatmap of amino acid concentrations for the pairwise comparison between Braak LB 6 and Ctrl. **E** Robust volcano plot for the Braak LB 6 *vs.* Ctrl comparison, displaying $\log_2$(FC) and $-\log_{10}$(*p*-value) and highlighting no significant variations in amino acid levels. Ctrl control, Braak LB Braak Lewy Body Stage, SFG superior frontal gyrus.

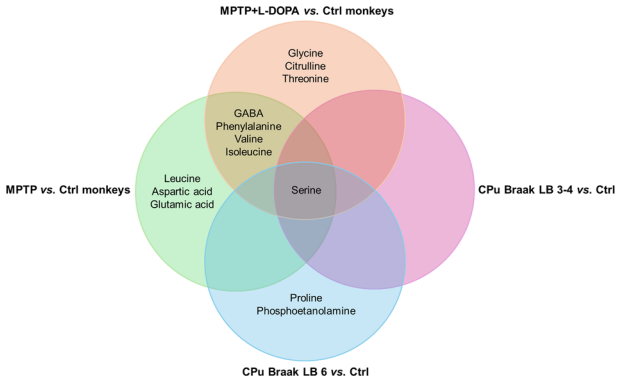

Fig. 6 | Overlapping and distinct amino acid alterations in the putamen of untreated and L-DOPA–treated MPTP-intoxicated macaques and in the caudate-putamen of PD patients across Braak Lewy body stages. The Venn diagram summarizes the amino acids dysregulated across all significant comparisons examined in the study, including the *post-mortem* putamen of untreated and L-DOPA–treated MPTP-intoxicated macaques, and the caudate-putamen of PD patients at different Braak Lewy body stages (Braak LB 3–4 and Braak LB 6 stages). Although the specific amino acid variation differed between macaques and PD patients, and across treatment- or stage-dependent conditions, serine consistently emerged as an upregulated amino acid across all analyses. Ctrl control, CPu caudate-putamen, Braak LB Braak Lewy Body Stage.

Consistent with our findings, previous studies have shown higher striatal GABA levels in untreated MPTP-intoxicated monkeys[52], as well as in patients with PD[50,53]. Considering that the CPu is made up of about the 90% of GABAergic medium spiny neurons[54], whose activity is regulated by nigrostriatal dopamine inputs[55–59], we argue that the upregulation of GABA biosynthesis might represent a compensatory mechanism in response to dopamine depletion, potentially aiming to restore the delicate balance of neuronal activity.

Previous reports have indicated reduced levels of citrulline in the sera[38] and CSF[60] of PD patients compared to controls. The increase in citrulline detected exclusively in the putamen of L-DOPA–treated MPTP-intoxicated macaques, reported in the present study, is of particular interest as citrulline is an intermediate of the urea cycle and a precursor of arginine and nitric oxide[61], both of which are critical for mitochondrial function and nitrosative stress—processes known to be disrupted in PD pathology[62,63].

Additionally, phenylalanine and BCAAs levels were found elevated in both untreated and L-DOPA–treated MPTP-intoxicated monkeys, while threonine was selectively increased in L-DOPA–treated animals, further suggesting widespread amino acid disturbances in the Parkinsonian brain. Notably, disturbances in BCAA metabolism are increasingly recognized as contributing to impaired energy production, mitochondrial dysfunction, oxidative stress, neuroinflammation, and altered glutamatergic neurotransmission[64]. By contrast, measurement of BCAAs levels in the CSF of PD patients has yielded mixed results, with one study reporting increased concentrations[65] and another reporting decreased levels[60] compared with controls.

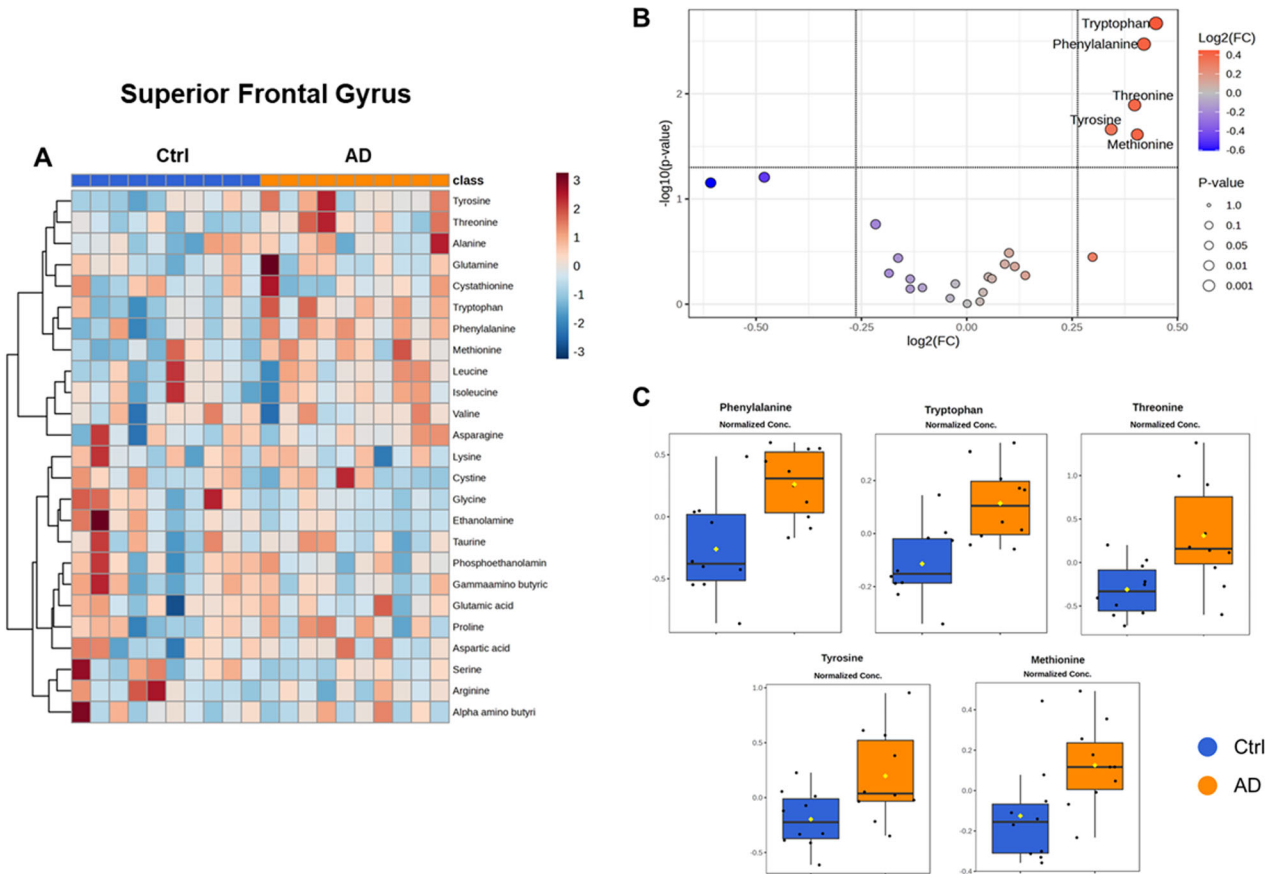

Fig. 7 | Amino acid alterations in the *post-mortem* superior frontal gyrus of Alzheimer's disease patients relative to controls. A Heatmap showing standardized amino acid concentrations (*z*-score) across AD ($n = 10$) and Ctrl ($n = 10$) groups. Rows represent individual amino acids and columns represent individual biological samples, highlighting the variation in amino acid levels. **B** Robust volcano plot for the AD *vs*. Ctrl, reporting $\log_2$(FC) and $-\log_{10}$(*p*-value) and identifying five significantly altered amino acids. **C** Boxplots depicting the amino acids significantly upregulated in AD relative to Ctrl. Ctrl control, AD Alzheimer's disease, SFG superior frontal gyrus.

Finally, the upregulation of glycine and serine is of considerable interest given their roles in neurotransmission and their involvement in various metabolic pathways, including antioxidant defense[66–68]. In this regard, findings from preclinical animal models and PD patients suggest that stimulation of the GluN1 subunit of glutamatergic NMDA receptors—where both glycine and D-serine bind—may confer therapeutic benefits in PD[69–72].

In contrast to the putamen, UPLC-MS analysis in SFG—a cortical region receiving dopaminergic innervations from the ventral tegmental area but not the substantia nigra pars compacta[73]—showed no significant changes in amino acid levels between MPTP-intoxicated monkeys and control monkeys, irrespective of L-DOPA treatment. These findings suggest that the amino acid metabolic alterations observed in PD brains are region-specific, predominantly affecting areas mostly impacted by dopaminergic denervation, such as the putamen.

The pronounced alterations in amino acid levels observed in the *post-mortem* putamen of MPTP-intoxicated monkeys prompted us to investigate whether similar changes were present in the CPu of PD patients, stratified by Braak LB stages (3–4 and 6). Unlike our observations in MPTP-intoxicated monkeys, UPLC-MS analysis in the *post-mortem* CPu of the entire cohort of PD patients revealed a significant alteration in only three amino acids—serine, phosphoethanolamine, and proline—compared to non-demented controls. Interestingly, increased levels of phosphoethanolamine and proline have been previously reported in the sera of PD patients[38,74], while the upregulation of serine is consistent with our earlier HPLC and metabolomic study conducted on *post-mortem* CPu and CSF samples from PD patients[21].

The differences in amino acid levels between patients with PD and MPTP-intoxicated monkeys are not surprising and can be attributed to several factors. These include sex-related heterogeneity, differential peripheral organ dysfunctions[75,76], as well as divergent disease aetiologies, progression rates, and compensation mechanisms, with monkeys developing severe neurodegeneration within months, in contrast to the years-long progression observed in patients. Another crucial factor concerns the *post-mortem* delay, which is minimal in monkeys (in the range of minutes) but substantially longer in patients (several hours). As highlighted by previous studies[77–79], metabolite levels can shift dramatically within seconds after death, as enzymatic activity continues to modify the biochemical profile. Moreover, in contrast to MPTP-intoxicated macaques subjected exclusively to L-DOPA treatment for months until the development of stable dyskinesia, PD patients examined in this work received L-DOPA therapy for years, often in combination with dopaminergic agonists, COMT and MAO inhibitors, anticholinergics, or amantadine, particularly during the final year of life (Supplementary Tables 1 and 2).

Interestingly, upon patient stratification by Braak LB stages, serine was the only amino acid found upregulated in patients at stages 3–4, whereas at stage 6, serine and proline were significantly upregulated while phosphoethanolamine was downregulated relative to non-demented controls.

When comparing PD patients at Braak LB stages 3–4 with those at stage 6, we found that arginine levels were significantly downregulated in patients at stage 6. Arginine is critically involved in the synthesis of nitric oxide, an important regulator of physiological processes in the brain, including synaptic plasticity, intracellular signaling, and cerebral blood flow[80]. Although the biochemical mechanisms underlying the progressive downregulation of arginine remain to be elucidated, interpretation of these

data should consider that the amino acid profile of PD patients may be partially influenced by the progressive disease-related increases in microglial and astrocytic populations[81], which shift tissue cellular composition and consequently alter the relative contribution of neuron- versus glia-derived metabolites in *post-mortem* samples. From a functional perspective, it is noteworthy that repeated systemic pre-treatment with L-arginine has been shown to prevent MPTP-induced dopaminergic cell loss in the substantia nigra pars compacta in mice[82].

When we extended the UPLC-MS analysis to *post-mortem* SFG, we failed to detect any statistically significant differences in amino acid concentrations between patients with PD and non-demented controls, a finding consistent with our results in untreated and L-DOPA-treated MPTP-intoxicated monkeys. Notably, the region-specific pattern of amino acid alterations shared between monkeys and humans indicates that, although this primate model has limitations in fully recapitulating the prolonged disease course and the complexity of pharmacological treatment in PD, it nonetheless provides strong validity for modeling complex metabolic alterations seen in patients with this neurodegenerative disease[83].

The present UPLC-MS analysis on the *post-mortem* brain of PD patients provides complementary information to prior meta-analyses of serum/plasma amino acids[7,23,33,38]. Whereas peripheral studies have identified broad amino acid alterations that distinguish PD patients from controls, changes in the CPu were restricted to fewer amino acids. This divergence likely reflects the distinct biological contexts captured by peripheral versus central measurements. Alterations in circulating amino acids may mirror multisystemic pathophysiological processes, whereas changes within the CPu are more likely to reflect local neuropathological features. Nonetheless, future studies with larger *post-mortem* cohorts and integration of additional OMIC approaches will be essential to clarify the biological relevance of these complementary metabolic signatures.

Notably, across all amino acids found to be altered in the putamen of MPTP-intoxicated monkeys, as well as in the CSF[21] and CPu of PD patients, serine is the only metabolite that consistently emerges. In this regard, it is noteworthy that serine exists in two distinct enantiomeric configurations, D- and L-serine, whose brain concentrations are strictly regulated and balanced due to their critical central effects. Specifically, while in the brain the atypical amino acid D-serine acts as a co-agonist of the NMDA receptor[68,84], L-serine serves as a metabolic precursor for sphingolipids, purine nucleotides, antioxidants, and NMDA receptor co-agonists (glycine and D-serine)[85,86]. Although UPLC-MS analysis does not allow for the discrimination of serine enantiomers, our previous HPLC studies demonstrated elevated levels of both D- and L-serine in brain tissue from experimental PD models, *post-mortem* brain samples from PD patients, and CSF from de novo PD patients compared to controls[21,46]. These convergent findings suggest a concomitant increase in both serine enantiomers. We hypothesize that elevation in CPu D-serine levels may reflect an adaptive NMDA receptor-related response aimed at contrasting the progressive loss of striatal dopamine signaling in PD. This hypothesis is supported by recent evidence demonstrating that D-serine modulates dopamine release in the CPu by enhancing glutamatergic transmission through NMDA receptors on dopaminergic nigrostriatal neurons[87]. Moreover, elevation of spinal D-serine levels, achieved through either genetic manipulation or exogenous D-serine administration, was found to attenuate motor symptoms, improve blood–brain barrier (BBB) function and permeability, and counteract neuroinflammation in the experimental autoimmune encephalomyelitis (EAE) mouse model of multiple sclerosis[88]. These findings are highly relevant, given that BBB disruption and neuroinflammation are well-established neuropathological mechanisms contributing to PD[89,90]. While further investigation is warranted, current evidence supports serine as a promising biomarker for PD and underscores the utility of its inclusion within broader multi-analyte panels designed to capture the complexity of the disease.

Lastly, we evaluated by UPLC-MS the amino acid metabolic profile in *post-mortem* SFG samples from controls and AD patients—a brain region known to be affected by this neurodegenerative disorder[35–37]. Through this approach, we aimed to evaluate the impact of different neurodegenerative conditions on cortical amino acid metabolism. Consistent with the known relevance of this brain region in AD, and in stark contrast to our findings in PD patients, we observed significant alterations in amino acid metabolism in the *post-mortem* SFG of patients with AD. Specifically, our data indicated a significant upregulation in the levels of tryptophan, phenylalanine, threonine, tyrosine, and methionine in AD patients compared to controls. These results align with previous reports documenting alterations in the metabolism of these amino acids in brain regions highly susceptible to AD pathology, such as the hippocampus[91], the Brodmann area 9—which is located within the SFG[91,92]—and the temporal cortex[93]. Notably, these findings underscore that amino acid level alterations in cortical regions such as the SFG are highly dependent on the underlying neuropathological condition, as clearly demonstrated by the divergent metabolic profiles observed in patients with PD and AD compared to controls.

While the present study extends our understanding of amino acid disruptions in the brains of PD and AD patients, the primary limitations of this study are the relatively small sample sizes of *post-mortem* brain tissue from both humans and non-human primates, as well as the imbalance between male and female subjects in both animal models and patient cohorts[27,29,94]. A further limitation is the inability to stratify patients by genetic background, which likely restricts the cohort to idiopathic cases due to the limited sample size. Such constraints arise from the inherent difficulty of obtaining *post-mortem* brain tissue samples from the study population. We also acknowledge that p-values were not adjusted for multiple comparisons, which may increase the risk of Type I errors. Therefore, the findings should be interpreted with caution. Nonetheless, the consistent alterations observed across disease stages and experimental groups support the biological relevance of the main results. At the same time, the study's primary strength lies in stratifying the PD cohort by Braak LB stages (3–4 vs. 6), thus providing direct insight into disease progression and employing targeted UPLC-MS for amino acid profiling, a platform frequently used in clinic renowned for its high sensitivity, selectivity, and quantitative accuracy in complex biological matrices.

In summary, the present UPLC-MS study identifies specific amino acid alterations in *post-mortem* brain samples of MPTP-intoxicated monkeys and PD patients as potential markers of cellular insult in the brain, which may be directly or indirectly linked to neurodegeneration. Notably, these amino acid alterations were numerically less widespread compared to those previously reported in the PD serum[7,14,23,33,38] and confined to the CPu, with serine being uniquely upregulated across both species and disease stages. In contrast, the amino-acid profile in the SFG remained unaltered in both MPTP-intoxicated monkeys and PD patients. Still, it exhibited distinct dysregulation in AD patients, thereby demonstrating disease- and region-specific metabolic signatures. Lastly, considering the critical role of serine as a metabolic precursor for sphingolipids, purine nucleotides, antioxidants, and NMDA-receptor co-agonists, these findings collectively suggest that serine accumulation may contribute to cellular adaptive processes associated with PD and support its inclusion in multi-analyte biomarker panels for PD.

Methods

Human post-mortem tissue collection

Post-mortem tissue samples from the caudate-putamen (CPu) of Parkinson's disease (PD) patients and the superior frontal gyrus (SFG) of PD and Alzheimer's disease (AD) patients were obtained from The Netherlands Brain Bank (Netherlands Institute for Neuroscience, Amsterdam; open access: www.brainbank.nl) and derived from three distinct cohorts of patients and corresponding non-demented control subjects. Specifically, CPu tissues derived from a cohort of 26 PD patients comprising 13 individuals classified as Braak Lewy body (LB) stage 3–4 and 13 individuals as Braak LB stage 6. Due to the limited availability of *post-mortem* CPu samples from controls, PD patients were compared with 6 non-demented controls matched for age, sex, and *post-mortem* interval (PMI) to minimize potential confounding effects in the statistical analysis. *Post-mortem* SFG samples were derived from a cohort of subjects consisting of patients with PD, AD,

and controls. The number of PD patients (Braak LB stage ≥4; $n = 10$) was comparable to that from non-demented controls ($n = 10$), as well as the number of AD patients (neuropathological staging of Braak ≥5; $n = 10$), and both PD and AD groups were matched with the control group for age, sex, and PMI. Non-demented controls were selected from adults with no cognitive decline and with a Braak LB score ≤3 in accordance with the Braak and Braak criteria[95]. Demographic characteristics of PD patients and non-demented controls are described in Table 1 (CPu). Demographic characteristics of the other cohorts, including patients with PD, AD, and non-demented controls, are described in Table 2 (SFG). Control subjects had no known clinical history of neurological or psychiatric disorders, as confirmed by neuropathological evaluation of their samples. The clinical diagnosis of PD was established according to the UK Brain Bank criteria[96], subsequently confirmed by neuropathological findings[97], and AD was diagnosed based on the National Institute of Neurological and Communicative Disorders and Stroke and the Alzheimer's Disease and Related Disorders Association (NINCDS-ADRDA) criteria[98]. Frozen CPu and SFG tissues were pulverized in liquid nitrogen and stored at −80 °C for subsequent processing. All material and data acquired by the Netherlands Brain Bank adhere to a strict protocol requiring written informed consent and were in conformity with the Helsinki Declaration. In instances where individuals are unable to provide informed consent due to health conditions, authorization is obtained from their legal representative, in accordance with the Netherlands Civil Code (Burgerlijk Wetboek). Additional details are available at: https://www.brainbank.nl/about-us/ethics/.

Table 1 | Demographic and clinical characteristics of Parkinson's disease patients and non-demented control subjects from *post-mortem* caudate-putamen samples

Characteristics	Control		Parkinson's disease	
	N	Median [IQR]	*N*	Median [IQR]
Subjects (total number)	6		26	
Gender (M / F)	1/5		16/10	
Age (years, median [IQR])		83.00 [74.50–86.00]		76.00 [67.00–81.00]
PMI (hours, median [IQR])		5.42 [4.86–6.69]		5.79 [5.00–6.83]
Braak LB stage(0-II/III/IV/V/VI)	0/0/0/0/0		0/3/10/0/13	

Values are expressed as median (interquartile range, IQR).
F female, *M* male, *N* numerosity, *PMI* post-mortem interval, *Braak LB* Braak Lewy body.

Non-human primates

Tissues used in the present study were obtained from an experimental brain bank, with detailed protocols described elsewhere[99–103]. Briefly, 1-methyl-4-phenyl-1,2,3,6-tetrahydropyridine (MPTP)-intoxicated non-human primate PD model macaques ($n = 9$) received daily intravenous injections of MPTP hydrochloride (0.2 mg/kg) until stable parkinsonian motor symptoms developed. Four (4) were kept free of dopamine replacement therapy (L-DOPA, dopamine agonist, inhibitor of monoamine oxidase, inhibitor of C-O-methyl transferase, etc.) until the L-DOPA-exposed group ($n = 5$) was terminated, i.e., they were maintained several months in the OFF state. These five (5) animals were administered individually titrated doses of L-DOPA (Madopar; L-DOPA/carbidopa, 4:1 ratio; range: 9–17 mg/kg), twice daily, to achieve optimal reversal of motor deficits. This treatment was maintained for 4–5 months until dyskinesia stabilized. Thereafter, L-DOPA was administered biweekly to sustain a consistent dyskinetic state prior to acute pharmacological testing. At the end of the study, animals were euthanized via intravenous overdose of sodium pentobarbital (150 mg/kg) one hour after the final administration of L-DOPA, and brains were rapidly extracted. A control group of five (5) macaques, not treated with MPTP hydrochloride or L-DOPA, was included as a control. Each brain was bisected along the midline, and both hemispheres were immediately frozen in isopentane at −45 °C, then stored at −80 °C. Coronal sections (300 µm thick) were cut using a cryostat, and tissue punches were obtained from the rostral putamen and the SFG. As previously reported[102], this experimental procedure induces a significant reduction (>75%) in striatal tyrosine hydroxylase protein expression and dopamine levels.

Ultra-performance liquid chromatography-mass spectrometry

Brain tissue samples from humans and monkeys were homogenized in 1:20 (w/v) 0.2 M trichloroacetic acid (TCA), sonicated (3 cycles, 10 s each), and centrifuged at 13,000 × *g* for 20 min. The TCA supernatants were used for subsequent analyses.

The concentrations of a panel of 44 amino acids and derivatives were measured in brain tissue extracts from Parkinsonian monkeys, patients with PD and AD, and their respective matched controls, using UPLC-MS. The panel includes: 1-Methylhistidine, 3-Methylhistidine, 4-Hydroxyproline, α-Aminobutyric acid, β-Alanine, β-Aminobutyric acid, γ-Aminobutyric acid, Alanine, Allo-Isoleucine, Aminoadipic acid, Anserine, Arginine, Asparagine, Aspartic acid, Carnosine, Citrulline, Cystathionine, Cystine, Ethanolamine, Glutamic acid, Glutamine, Glycine, Glycil proline, Histidine, Homocitrulline, Homocystine, Hydroxylysine, Isoleucine, Kynurenine, Leucine, Lysine, Methionine, Ornithine, Phenylalanine, Phosphoethanolamine, Proline, Sarcosine, Serine, Sulfocysteine, Taurine, Threonine, Tryptophan, Tyrosine, Valine.

Table 2 | Demographic and clinical characteristics of Alzheimer's disease, Parkinson's disease patients, and non-demented control subjects from *post-mortem* superior frontal gyrus samples

Characteristics	Control		Alzheimer's disease		Parkinson's disease	
	N	Median [IQR]	*N*	Median [IQR]	*N*	Median [IQR]
Subjects (total number)	10		10		10	
Gender (M / F)	10/0		10/0		10/0	
Age (years, median [IQR])		85.00 [79.00–88.25]		85.50 [82.00–88.00]		85.00 [81.75–86.00]
PMI (hours, median [IQR])		5.87 [5.62–6.58]		5.37 [5.04–6.42]		5.79 [4.42–6.45]
Braak stage (0-I/II-IV/V-VI)	3/7/0		0/0/10		3/7/0	
Braak LB stage (0-II/III/IV/V/VI)	4/0/0/0/0				0/0/2/2/6	

Values are expressed as median (interquartile range, IQR).
F female, *M* male, *N* numerosity, *PMI* post-mortem interval, *Braak LB* Braak Lewy body.

Sample preparation was performed by adding 50 µL of the sample to 100 µL 10% (w/v) sulfosalicylic acid containing an internal standard mix (50 µM) (Cambridge Isotope Laboratories, Inc., Tewksbury, MA, USA). The mixture was vortexed and then centrifuged at 10,000 rpm for 15 min. In a 1.5 mL vial, 70 µL of borate buffer and 20 µL of AccQ Tag reagents (Waters Corporation, Milford, MA, USA) were added to 10 µL of the obtained supernatant and heated at 55 °C for 10 min in a water bath. Next, samples were loaded onto a CORTECS UPLC C18 column 1.6 µm, 2.1 mm × 150 mm (Waters Corporation) for chromatographic separation (ACQUITY H-Class, Waters Corporation). Elution was accomplished at 0.5 mL/min flow-rate with a linear gradient (9 min) from 99:1 to 1:99 water 0.1% formic acid/acetonitrile 0.1% formic acid. Injection volume was 2 µL, and column oven temperature was set at 55 °C. Analytes were detected on an ACQUITY QDa single quadrupole mass spectrometer equipped with an electrospray source operating in positive ion mode (Waters Corporation).

The analytical process was monitored using amino acid controls (level 1 and level 2) manufactured by the MCA laboratory of the Queen Beatrix Hospital (The Netherlands). Amino acid concentrations were determined by comparison with values obtained from a standard curve for each amino acid (2,5–10–50–125–250–500 µmol/L only for Cysteine, 5–20–100–250–500–1000 µmol/L for all amino acids). For data analysis (calibration curves and amino acid quantitation), the instrument software TargetLynx was used.

Statistical analysis

UPLC-MS data were processed to construct four datasets. The macaque model putamen dataset was obtained from the *post-mortem* putamen of untreated MPTP-intoxicated macaques ($n = 4$), L-DOPA-treated MPTP-intoxicated macaques ($n = 5$), and untreated controls ($n = 5$). The macaque model SFG dataset was obtained from the *post-mortem* SFG of untreated MPTP-intoxicated macaques ($n = 4$), L-DOPA-treated MPTP-intoxicated macaques ($n = 5$), and untreated controls ($n = 5$). The CPu human dataset was obtained from the *post-mortem* CPu of PD patients ($n = 26$) and non-demented controls ($n = 6$). The CPu samples of PD patients were further divided based on the Braak LB stages (3–4 and 6). The SFG human dataset was obtained from the *post-mortem* SFG of PD patients ($n = 10$), AD patients ($n = 10$), and non-demented controls ($n = 10$). For the PD relative to controls analysis, the SFG samples of PD patients were further divided based on the Braak LB stages (4–5 and 6). The following conditions were applied for variables (amino acids) inclusion in every dataset: amino acids that were not detected or had more than 30% of missing values (m.v.) were excluded. The remaining m.v. were then imputed using the Probabilistic Principal Component Analysis (PPCA) method. The final set of amino acids included in each dataset is reported in Supplementary Table 3.

All the quantified amino acids were first normalized for protein concentration (nmol/mg). Then, datasets were normalized according to the specific data distribution. The macaque model datasets were log-transformed and auto-scaled, while the CPu and SFG human datasets were normalized by median and Pareto scaling. Differential amino acid levels were obtained using a fold change (FC) threshold set at 1.2. Statistical significance was assessed using a *t*-test with significance defined as p-value < 0.05. Given the limited availability of non-human primate and human brain tissue, the achievable sample sizes were necessarily small; under these conditions, strict multiple-testing correction procedures were not applied to avoid reducing statistical power and the risk of obscuring biologically relevant effects. Volcano plots were created using FC = 1.2 and p-value < 0.05 as thresholds. All statistical analyses, heatmaps, volcano plots, and box plots were generated using MetaboAnalyst 6.0 (http://www.metaboanalyst.ca/). For the construction of the heatmaps, normalized amino acid data were used. Hierarchical clustering was applied to the amino acids using Euclidean distance and Ward's linkage method.

Data availability

The raw data supporting the findings of the present study are available on request from the corresponding author.

Received: 24 September 2025; Accepted: 19 February 2026;
Published online: 04 March 2026

References

1. Zhu, J. et al. Temporal trends in the prevalence of Parkinson's disease from 1980 to 2023: a systematic review and meta-analysis. *Lancet Healthy Longev.* **5**, e464–e479 (2024).
2. Obeso, J. A. et al. Past, present, and future of Parkinson's disease: a special essay on the 200th Anniversary of the Shaking Palsy. *Mov. Disord.* **32**, 1264–1310 (2017).
3. Wüllner, U. et al. The heterogeneity of Parkinson's disease. *J. Neural Transm.* **130**, 827–838 (2023).
4. Greenland, J. C., Williams-Gray, C. H. & Barker, R. A. The clinical heterogeneity of Parkinson's disease and its therapeutic implications. *Eur. J. Neurosci.* **49**, 328–338 (2019).
5. Yilmaz, R., Hopfner, F., van Eimeren, T. & Berg, D. Biomarkers of Parkinson's disease: 20 years later. *J. Neural Transm.* **126**, 803–813 (2019).
6. Yamashita, K. Y., Bhoopatiraju, S., Silverglate, B. D. & Grossberg, G. T. Biomarkers in Parkinson's disease: a state of the art review. *Biomark. Neuropsychiatry* **9**, 100074 (2023).
7. Havelund, J. F., Heegaard, N. H. H., Færgeman, N. J. K. & Gramsbergen, J. B. Biomarker research in Parkinson's disease using metabolite profiling. *Metabolites* **7**, 42 (2017).
8. Li, X., Fan, X., Yang, H. & Liu, Y. Review of metabolomics-based biomarker research for Parkinson's disease. *Mol. Neurobiol.* **59**, 1041–1057 (2022).
9. Carrillo, F. et al. Multiomics approach discloses lipids and metabolites profiles associated to Parkinson's disease stages and applied therapies. *Neurobiol. Dis.* **202**, 106698 (2024).
10. Gonzalez-Riano, C. et al. Prognostic biomarkers of Parkinson's disease in the Spanish EPIC cohort: a multiplatform metabolomics approach. *Npj Parkinsons Dis.* **7**, 73 (2021).
11. Hu, L. et al. Integrated metabolomics and proteomics analysis reveals plasma lipid metabolic disturbance in patients with Parkinson's disease. *Front. Mol. Neurosci.* **13**, 80 (2020).
12. Meoni, G. et al. Metabolite and lipoprotein profiles reveal sex-related oxidative stress imbalance in de novo drug-naive Parkinson's disease patients. *Npj Parkinsons Dis.* **8**, 14 (2022).
13. Trupp, M. et al. Metabolite and peptide levels in plasma and CSF differentiating healthy controls from patients with newly diagnosed Parkinson's disease. *J. Parkinsons Dis.* **4**, 549–560 (2014).
14. Gervasoni, J. et al. Independent serum metabolomics approaches identify disrupted glutamic acid and serine metabolism in Parkinson's disease patients. *Npj Parkinsons Dis*. **11**, 274 (2025).
15. Kumari, S. et al. Quantitative metabolomics of saliva using proton NMR spectroscopy in patients with Parkinson's disease and healthy controls. *Neurol. Sci.* **41**, 1201–1210 (2020).
16. Shao, Y. et al. Comprehensive metabolic profiling of Parkinson's disease by liquid chromatography-mass spectrometry. *Mol. Neurodegener.* **16**, 4 (2021).
17. Bogdanov, M. et al. Metabolomic profiling to develop blood biomarkers for Parkinson's disease. *Brain* **131**, 389–396 (2008).
18. Huang, W. et al. Metabolomics-driven identification of adenosine deaminase as therapeutic target in a mouse model of Parkinson's disease. *J. Neurochem.* **150**, 282–295 (2019).
19. LeWitt, P. A., Li, J., Lu, M., Guo, L. & Auinger, P. Metabolomic biomarkers as strong correlates of Parkinson disease progression. *Neurology* **88**, 862–869 (2017).
20. Chang, K.-H. et al. Alterations of sphingolipid and phospholipid pathways and ornithine level in the plasma as biomarkers of Parkinson's disease. *Cells* **11**, 395 (2022).
21. Di Maio, A. et al. Homeostasis of serine enantiomers is disrupted in the post-mortem caudate putamen and cerebrospinal fluid of

living Parkinson's disease patients. *Neurobiol. Dis.* **184**, 106203 (2023).
22. Imarisio, A. et al. Blood D-serine levels correlate with aging and dopaminergic treatment in Parkinson's disease. *Neurobiol. Dis.* **192**, 106413 (2024).
23. Jiménez-Jiménez, F. J., Alonso-Navarro, H., García-Martín, E. & Agúndez, J. A. G. Cerebrospinal and blood levels of amino acids as potential biomarkers for Parkinson's disease: review and meta-analysis. *Eur. J. Neurol.* **27**, 2336–2347 (2020).
24. Figura, M. et al. Serum amino acid profile in patients with Parkinson's disease. *PLoS ONE* **13**, e0191670 (2018).
25. Plewa, S. et al. The metabolomic approach reveals the alteration in human serum and cerebrospinal fluid composition in Parkinson's disease patients. *Pharmaceuticals* **14**, 935 (2021).
26. Toczylowska, B., Zieminska, E., Michałowska, M., Chalimoniuk, M. & Fiszer, U. Changes in the metabolic profiles of the serum and putamen in Parkinson's disease patients – in vitro and in vivo NMR spectroscopy studies. *Brain Res.* **1748**, 147118 (2020).
27. Yahyavi, I. et al. Differences in sex and genetic status affect the disruption of NMDAR-related amino acid homeostasis in Parkinson's disease. Preprint at https://doi.org/10.1101/2025.08.08.25333287 (2025).
28. Nuzzo, T. et al. Deep brain stimulation rescues the homeostasis disruption of circulating D- and L-amino acids level in men with Parkinson's disease. *Neurobiol. Dis.* **216**, 107150 (2025).
29. Marino, C. et al. Untargeted 1H NMR-based metabolomics reveal sex-based differences in blood metabolome profiles among patients with Parkinson's disease, regardless of their idiopathic or genetic subtype. Preprint at https://doi.org/10.1101/2025.10.30.25339159 (2025).
30. Marino, C. et al. Untargeted 1H NMR-based metabolomics and high-pressure liquid chromatography analysis reveal sexual dimorphism in the serum metabolic profiles of Parkinson's disease patients harbouring rare genetic variants. Preprint at https://doi.org/10.1101/2025.11.20.25340670 (2025).
31. Peng, H. et al. Association between kidney function and Parkinson's disease risk: a prospective study from the UK Biobank. *BMC Public Health* **24**, 2225 (2024).
32. Reyes, J. F. et al. Accumulation of alpha-synuclein within the liver, potential role in the clearance of brain pathology associated with Parkinson's disease. *Acta Neuropathol. Commun.* **9**, 46 (2021).
33. Luo, X., Liu, Y., Balck, A., Klein, C. & Fleming, R. M. T. Identification of metabolites reproducibly associated with Parkinson's Disease via meta-analysis and computational modelling. *Npj Parkinsons Dis.* **10**, 1–17 (2024).
34. Bezard, E. et al. Modeling Parkinson's disease in primates. *Cold Spring Harb. Perspect. Med.* **15**, a041612 (2025).
35. Fujimoto, H. et al. Brain regions associated with anosognosia for memory disturbance in Alzheimer's disease: a magnetic resonance imaging study. *Neuropsychiatr. Dis. Treat.* **ume 13**, 1753–1759 (2017).
36. Lee, D. Y. et al. Frontal dysfunction underlies depressive syndrome in Alzheimer disease: a FDG-PET study. *Am. J. Geriatr. Psychiatry* **14**, 625–628 (2006).
37. Yuan, Y., Chen, Y. P., Boyd-Kirkup, J., Khaitovich, P. & Somel, M. Accelerated aging-related transcriptome changes in the female prefrontal cortex. *Aging Cell* **11**, 894–901 (2012).
38. Akdas, S., Yuksel, D. & Yazihan, N. Assessment of the relationship between amino acid status and Parkinson's disease: a comprehensive review and meta-analysis. *Can. J. Neurol. Sci.* https://doi.org/10.1017/cjn.2024.310 (2024).
39. Basellini, M. J. et al. Pathological pathways and alpha-synuclein in Parkinson's disease: a view from the periphery. *Front. Biosci.* **28**, 33 (2023).
40. Choi, J.-H. et al. Clinical perspectives of Parkinson's disease for ophthalmologists, otorhinolaryngologists, cardiologists, dentists, gastroenterologists, urologists, physiatrists, and psychiatrists. *J. Korean Med. Sci.* **35**, e230 (2020).
41. Ma, L.-Y. et al. Alpha-synuclein in peripheral tissues in Parkinson's disease. *ACS Chem. Neurosci.* **10**, 812–823 (2019).
42. Titova, N., Padmakumar, C., Lewis, S. J. G. & Chaudhuri, K. R. Parkinson's: a syndrome rather than a disease? *J. Neural Transm.* **124**, 907–914 (2017).
43. Gardoni, F. & Di Luca, M. Targeting glutamatergic synapses in Parkinson's disease. *Curr. Opin. Pharmacol.* **20**, 24–28 (2015).
44. Almohmadi, N. H. et al. Glutamatergic dysfunction in neurodegenerative diseases focusing on Parkinson's disease: Role of glutamate modulators. *Brain Res. Bull.* **225**, 111349 (2025).
45. Carvajal, F. J., Mattison, H. A. & Cerpa, W. Role of NMDA receptor-mediated glutamatergic signaling in chronic and acute neuropathologies. *Neural Plast.* **2016**, 2701526 (2016).
46. Serra, M. et al. Perturbation of serine enantiomers homeostasis in the striatum of MPTP-lesioned monkeys and mice reflects the extent of dopaminergic midbrain degeneration. *Neurobiol. Dis.* **184**, 106226 (2023).
47. Gerlach, M. et al. A post mortem study on neurochemical markers of dopaminergic, GABA-ergic and glutamatergic neurons in basal ganglia-thalamocortical circuits in Parkinson syndrome. *Brain Res.* **741**, 142–152 (1996).
48. Rinne, J. O., Halonen, T., Riekkinen, P. J. & Rinne, U. K. Free amino acids in the brain of patients with Parkinson's disease. *Neurosci. Lett.* **94**, 182–186 (1988).
49. Perry, T. L., Javoy-Agid, F., Agid, Y. & Fibiger, H. C. Striatal GABAergic neuronal activity is not reduced in Parkinson's disease. *J. Neurochem.* **40**, 1120–1123 (1983).
50. Kish, S. J. et al. Elevated gamma-aminobutyric acid level in striatal but not extrastriatal brain regions in Parkinson's disease: correlation with striatal dopamine loss. *Ann. Neurol.* **20**, 26–31 (1986).
51. Porras, G. et al. L-dopa-induced dyskinesia: beyond an excessive dopamine tone in the striatum. *Sci. Rep.* **4**, 3730 (2014).
52. Boulet, S. et al. Behavioral recovery in MPTP-treated monkeys: neurochemical mechanisms studied by intrastriatal microdialysis. *J. Neurosci.* **28**, 9575–9584 (2008).
53. O'Gorman Tuura, R. L., Baumann, C. R. & Baumann-Vogel, H. Beyond dopamine: GABA, glutamate, and the axial symptoms of Parkinson disease. *Front. Neurol.* **9**, 806 (2018).
54. Alexander, G. E. & Crutcher, M. D. Functional architecture of basal ganglia circuits: neural substrates of parallel processing. *Trends Neurosci.* **13**, 266–271 (1990).
55. Andreoli, L., Abbaszadeh, M., Cao, X. & Cenci, M. A. Distinct patterns of dyskinetic and dystonic features following D1 or D2 receptor stimulation in a mouse model of Parkinsonism. *Neurobiol. Dis.* **157**, 105429 (2021).
56. Borroto-Escuela, D. O. et al. Brain dopamine transmission in health and Parkinson's disease: modulation of synaptic transmission and plasticity through volume transmission and dopamine heteroreceptors. *Front. Synaptic Neurosci*. **10**, 20 (2018).
57. Florio, E. et al. D2R signaling in striatal spiny neurons modulates L-DOPA induced dyskinesia. *iScience* **25**, 105263 (2022).
58. Sáez, M. et al. D2 dopamine receptors and the striatopallidal pathway modulate L-DOPA-induced dyskinesia in the mouse. *Neurobiol. Dis.* **186**, 106278 (2023).
59. Shen, W., Flajolet, M., Greengard, P. & Surmeier, D. J. Dichotomous dopaminergic control of striatal synaptic plasticity. *Science* **321**, 848–851 (2008).
60. Molina, J. A. et al. Decreased cerebrospinal fluid levels of neutral and basic amino acids in patients with Parkinson's disease. *J. Neurol. Sci.* **150**, 123–127 (1997).

61. Papadia, C., Osowska, S., Cynober, L. & Forbes, A. Citrulline in health and disease. Review on human studies. *Clin. Nutr.* **37**, 1823–1828 (2018).
62. Henrich, M. T., Oertel, W. H., Surmeier, D. J. & Geibl, F. F. Mitochondrial dysfunction in Parkinson's disease – a key disease hallmark with therapeutic potential. *Mol. Neurodegener.* **18**, 83 (2023).
63. Stykel, M. G. & Ryan, S. D. Nitrosative stress in Parkinson's disease. *Npj Parkinsons Dis.* **8**, 104 (2022).
64. Huang, H.-Y. et al. Branched-chain amino acids in Parkinson's disease: molecular mechanisms and therapeutic potential. *Int. J. Mol. Sci*. **26**, 6992 (2025).
65. Wuolikainen, A. nna et al. Multi-platform mass spectrometry analysis of the CSF and plasma metabolomes of rigorously matched amyotrophic lateral sclerosis, Parkinson's disease and control subjects. *Mol. Biosyst.* **12**, 1287–1298 (2016).
66. Johnson, A. A. & Cuellar, T. L. Glycine and aging: evidence and mechanisms. *Ageing Res. Rev.* **87**, 101922 (2023).
67. Wolosker, H. The neurobiology of d-serine signaling. *Adv. Pharmacol.* **82**, 325–348 (2018).
68. Wolosker, H., Balu, D. T. & Coyle, J. T. The rise and fall of the d-serine-mediated gliotransmission hypothesis. *Trends Neurosci* **39**, 712–721 (2016).
69. Frouni, I. et al. Effect of glycine transporter 1 inhibition with bitopertin on Parkinsonism and L-DOPA induced dyskinesia in the 6-OHDA-lesioned rat. *Eur. J. Pharmacol.* **929**, 175090 (2022).
70. Frouni, I. et al. Effect of the glycine transporter 1 inhibitor ALX-5407 on dyskinesia, psychosis-like behaviours and Parkinsonism in the MPTP-lesioned marmoset. *Eur. J. Pharmacol.* **910**, 174452 (2021).
71. Gelfin, E. et al. D-serine adjuvant treatment alleviates behavioural and motor symptoms in Parkinson's disease. *Int. J. Neuropsychopharmacol.* **15**, 543–549 (2012).
72. Schmitz, Y. et al. Glycine transporter-1 Inhibition promotes striatal axon sprouting via NMDA receptors in dopamine neurons. *J. Neurosci.* **33**, 16778–16789 (2013).
73. Coenen, V. A. et al. The anatomy of the human medial forebrain bundle: ventral tegmental area connections to reward-associated subcortical and frontal lobe regions. *NeuroImage Clin* **18**, 770–783 (2018).
74. Picca, A. et al. Circulating amino acid signature in older people with Parkinson's disease: a metabolic complement to the EXosomes in PArkiNson Disease (EXPAND) study. *Exp. Gerontol.* **128**, 110766 (2019).
75. Delamarre, A. et al. Gastrointestinal and metabolic function in the MPTP-treated macaque model of Parkinson's disease. *Heliyon* **6**, e05771 (2020).
76. Goldstein, D. S., Li, S.-T., Holmes, C. & Bankiewicz, K. Sympathetic Innervation in the 1-Methyl-4-phenyl-1,2,3,6-tetrahydropyridine primate model of Parkinson's disease. *J. Pharmacol. Exp. Ther.* **306**, 855–860 (2003).
77. Scholefield, M. et al. Effects of alterations of post-mortem delay and other tissue-collection variables on metabolite levels in human and rat brain. *Metabolites* **10**, 438 (2020).
78. Zissler, A. et al. Influencing factors on postmortem protein degradation for PMI estimation: a systematic review. *Diagnostics* **11**, 1146 (2021).
79. Dienel, G. A. & Nowak, Jr, T. S. Setting standards for brain collection procedures in metabolomic studies. *J. Cereb. Blood Flow Metab*. https://doi.org/10.1177/0271678X251314331 (2025).
80. Virarkar, M., Alappat, L., Bradford, P. G. & Awad, A. B. L-arginine and nitric oxide in CNS function and neurodegenerative diseases. *Crit. Rev. Food Sci. Nutr.* **53**, 1157–1167 (2013).
81. Zaman, V. et al. Cellular and molecular pathophysiology in the progression of Parkinson's disease. *Metab. Brain Dis.* **36**, 815–827 (2021).
82. Hami, J. et al. Effects of L-arginine pre-treatment in 1-methyl-4-phenyl-1,2,3,6-tetrahydropyridine-induced Parkinson's diseases in Balb/c mice. *Iran. J. Neurol.* **14**, 195–203 (2015).
83. Bezard, E. et al. Position paper: leveraging non-human primate (NHP) specificities to accelerate Parkinson's disease and ageing research. *Npj Parkinsons Dis.* **11**, 227 (2025).
84. Osaki, A. et al. Endogenous d-serine exists in the mammalian brain independent of synthesis by serine racemase. *Biochem. Biophys. Res. Commun.* **641**, 186–191 (2023).
85. Holm, L. J. & Buschard, K. L-serine: a neglected amino acid with a potential therapeutic role in diabetes. *APMIS* **127**, 655–659 (2019).
86. Murtas, G., Marcone, G. L., Sacchi, S. & Pollegioni, L. L-serine synthesis via the phosphorylated pathway in humans. *Cell. Mol. Life Sci.* **77**, 5131–5148 (2020).
87. Ringlet, S. et al. Glycine-gated extrasynaptic NMDARs activated during glutamate spillover drive burst firing in nigral dopamine neurons. *Prog. Neurobiol.* **249**, 102773 (2025).
88. Usiello, A. et al. Chiral shift toward D-serine reflects intrathecal inflammation in multiple sclerosis and counteracts motor impairment in a murine model. Preprint at https://doi.org/10.1101/2025.05.07.652561 (2025).
89. Lau, K., Kotzur, R. & Richter, F. Blood–brain barrier alterations and their impact on Parkinson's disease pathogenesis and therapy. *Transl. Neurodegener.* **13**, 37 (2024).
90. Tansey, M. G. et al. Inflammation and immune dysfunction in Parkinson disease. *Nat. Rev. Immunol.* **22**, 657–673 (2022).
91. Sordillo, L. A., Sordillo M.D., P. P. & Alfano, R. R. Abnormal tryptophan metabolism in Alzheimer's disease (ALZ): label-free spectroscopy suggests an alternative theory of ALZ causation. In *Optical Biopsy XVIII*: *Toward Real-Time Spectroscopic Imaging and Diagnosis* **11234**, 135–139 (SPIE, 2020).
92. Ambeskovic, M. et al. Metabolomic signatures of Alzheimer's disease indicate brain region-specific neurodegenerative progression. *Int. J. Mol. Sci.* **24**, 14769 (2023).
93. Gueli, M. C. & Taibi, G. Alzheimer's disease: amino acid levels and brain metabolic status. *Neurol. Sci.* **34**, 1575–1579 (2013).
94. Meoni, S., Macerollo, A. & Moro, E. Sex differences in movement disorders. *Nat. Rev. Neurol.* **16**, 84–96 (2020).
95. Braak, H. & Braak, E. Neuropathological stageing of Alzheimer-related changes. *Acta Neuropathol.* **82**, 239–259 (1991).
96. Hughes, A. J., Daniel, S. E., Kilford, L. & Lees, A. J. Accuracy of clinical diagnosis of idiopathic Parkinson's disease: a clinico-pathological study of 100 cases. *J. Neurol. Neurosurg. Psychiatry* **55**, 181–184 (1992).
97. Braak, H. & Braak, E. Staging of Alzheimer's disease-related neurofibrillary changes. *Neurobiol. Aging* **16**, 271–278 (1995).
98. McKhann, G. et al. Clinical diagnosis of Alzheimer's disease: report of the NINCDS-ADRDA Work Group under the auspices of Department of Health and Human Services Task Force on Alzheimer's Disease. *Neurology* **34**, 939–944 (1984).
99. Bezard, E. et al. μ opioid receptor agonism for L-DOPA-induced dyskinesia in Parkinson's disease. *J. Neurosci.* **40**, 6812–6819 (2020).
100. Engeln, M., De Deurwaerdère, P., Li, Q., Bezard, E. & Fernagut, P.-O. Widespread monoaminergic dysregulation of both motor and non-motor circuits in Parkinsonism and dyskinesia. *Cereb. Cortex* **25**, 2783–2792 (2015).
101. Hulme, H. et al. Basal ganglia neuropeptides show abnormal processing associated with L-DOPA-induced dyskinesia. *Npj Parkinsons Dis.* **8**, 1–11 (2022).
102. Nuzzo, T. et al. The levels of the NMDA receptor co-agonist D-serine are reduced in the substantia nigra of MPTP-lesioned macaques and in the cerebrospinal fluid of Parkinson's disease patients. *Sci. Rep.* **9**, 8898 (2019).

103. Santini, E. et al. Distinct changes in cAMP and extracellular signal-regulated protein kinase signalling in L-DOPA-induced dyskinesia. *PLoS ONE* **5**, e12322 (2010).

Acknowledgements

Post-mortem human caudate-putamen and superior frontal gyrus samples were provided by The Netherlands Brain Bank (Netherlands Institute for Neuroscience, Amsterdam, open access: www.brain bank.nl). We acknowledge Alessia Casamassa, Mattia Miroballo, Giorgia Donati, Giulia Sansone, Giada Torresi, and Martina Garofalo for their technical support. The authors also sincerely thank Dr. Matteo Vidali for his scientific advice during the revision of this manuscript. This study was partially funded by the Italian Ministry of University and Research (PRIN 2022 - COD. 2022XF7YYL_02 to AU). The work of A.U. and T.N. was supported by NEXTGENERATIONEU (NGEU) and funded by the Ministry of University and Research (MUR), National Recovery and Resilience Plan (NRRP), project MNESYS (PE0000006) – A Multiscale integrated approach to the study of the nervous system in health and disease (DN. 1553 11.10.2022).

Author contributions

J.G.: Data curation, Formal analysis, Investigation; A.D.M.: Investigation; M.S.: Writing – original draft, Writing – Critical revision & editing; L.S.: Investigation; M.C.: Data curation, Formal analysis; T.N.: Critical revision & editing; Q.L.: Investigation; M.L.T.: Investigation; M.M.: Critical revision; F.E.: Critical revision & editing; An.U.: Data curation, Formal analysis; E.B.: Critical revision & editing; A.U.: Conceptualization, Data curation, Funding acquisition, Project administration, Supervision, Visualization, Writing – original draft, Writing – Critical review and editing.

Competing interests

The authors declare no competing interests.

Additional information

Supplementary information The online version contains supplementary material available at https://doi.org/10.1038/s41531-026-01306-x.

Correspondence and requests for materials should be addressed to Alessandro Usiello.

Reprints and permissions information is available at http://www.nature.com/reprints

Publisher's note Springer Nature remains neutral with regard to jurisdictional claims in published maps and institutional affiliations.

Open Access This article is licensed under a Creative Commons Attribution-NonCommercial-NoDerivatives 4.0 International License, which permits any non-commercial use, sharing, distribution and reproduction in any medium or format, as long as you give appropriate credit to the original author(s) and the source, provide a link to the Creative Commons licence, and indicate if you modified the licensed material. You do not have permission under this licence to share adapted material derived from this article or parts of it. The images or other third party material in this article are included in the article's Creative Commons licence, unless indicated otherwise in a credit line to the material. If material is not included in the article's Creative Commons licence and your intended use is not permitted by statutory regulation or exceeds the permitted use, you will need to obtain permission directly from the copyright holder. To view a copy of this licence, visit http://creativecommons.org/licenses/by-nc-nd/4.0/.

© The Author(s) 2026